Covalent Functionalization of Multiwalled Carbon Nanotubes with a Low Molecular Weight Chitosan

Gang Ke,[†] Wenchao Guan,*[,†,‡] Changyu Tang,[†] Wenjie Guan,[§] Danlin Zeng,[||] and Feng Deng[||]

Department of Chemistry, Huazhong University of Science and Technology, Wuhan 430074, China, Key Laboratory of Cellulose and Lignocellulosics Chemistry, Guangzhou Institute of Chemistry, Chinese Academy of Sciences, P.O. Box 1122, Guangzhou Leyiju, China, Department of Physics, Wuhan University, Wuhan 430072, China, and State Key Laboratory of Magnetic Resonance and Atomic and Molecular Physics, Wuhan Institute of Physics and Mathematics, Chinese Academy of Sciences, Wuhan 430071, China

Received April 28, 2006; Revised Manuscript Received November 21, 2006

Covalent functionalization of shortened multiwalled carbon nanotubes (MWNTs) with a natural low molecular weight chitosan (LMCS) was accomplished by a nucleophilic substitution reaction. Amino and primary hydroxyl groups of the LMCS contributed mainly to the formation of MWNT−LMCS conjugates. The LMCS content in the MWNT−LMCS is approximately 58 wt %, and approximately four molecular chains of the LMCS are attached to 1000 carbon atoms of the nanotube sidewalls. Most interestingly, the amorphous packing structure of the LMCS changed dramatically when it attached to the MWNTs. The MWNTs might induce the crystalline character of the LMCS. As a novel derivative of MWNTs, the MWNT−LMCS is soluble in dimethylformamide, dimethyl acetamide, dimethylsulfoxide, and acetic acid aqueous solution. The confirmation of the chitosan-based covalent functionalization route might lead to further studies aiming for potential applications in catalysis and environmental protection.

Introduction

In recent years, covalent and noncovalent functionalizations of carbon nanotubes (CNTs) with polymers have been of significant interest.[1] The polymer-functionalization strategy is not only an effective way to solubilization of CNTs but also particularly important to the preparation of polymeric carbon nanocomposites.[2] By comparison, covalent methods have several advantages: (i) a broad range of polymers are available for use;[3] (ii) linkages between the nanotubes and the polymers are more stable and effective;[4] (iii) nanotube−polymer conjugates exhibit a higher solubility even with a relatively low degree of functionalization;[3] (iv) the versatility of polymer chemistry offers chemists flexible and efficient routes of synthesis.[5] Further, the covalent techniques allow the combination of different polymers with the CNTs to create new compound classes with unprecedented properties.[3−5] To achieve this, it is essential to functionalize the CNTs with ideal polymers.

Thus far, most of the studies focused on synthetic polymers, and various novel nanocomposites have been developed.[2−6] However, these polymers are generally derived from nonrenewable and increasingly finite fossil resources, and some bear toxic aromatic rings.[6]

Chitosan, a copolymer of 2-amino-2-deoxy-β-D-glucopyranose and 2-acetamido-2-deoxy-β-D-glucopyranose, is the deacetylated derivative of chitin, the second most abundant natural polymer on earth.[7] As opposed to easily accessible anionic polysaccharides, chitosan is a unique cationic polysaccharide and thus has attracted particular attention since the late 1970s.[8] Along with the development of chitosan science, chitosan and its many derivatives, which combine nontoxicity, biocompatibility, biodegradability, and bioactivity with attractive physical and mechanical properties, are becoming increasingly important.[9] Consequently, they have broad applications in metal chelating agents, medicine, pharmaceutics, food additives, antimicrobial agents, adhesives, textiles, etc.[10]

Due to its metal binding ability, effective removal of toxic pollutants is a large-scale use of chitosan.[9,11] Moreover, this chelating ability makes chitosan a potential candidate for a catalyst support.[12] Similarly, previous results have shown that CNTs are not only an efficient adsorbent for removal of cadmium(II), lead(II), etc. but also attractive supports for metal and metal oxide catalysts, owing to the unique structure and properties of the CNTs.[13,14] Thus, both materials share some important properties; the opportunity to combine CNTs and chitosan appears as a desirable way to develop environmentally friendly nanocomposites provided with properties that are inherent in both components.

As a basis of further studies aiming for potential applications in catalysis and environmental protection, it is urgent to create functional multiwalled carbon nanotubes (MWNTs) with chitosan. In this communication, we report the first successful covalent functionalization of shortened MWNTs with a water-soluble low molecular weight chitosan (LMCS, $\bar{M}_w \approx 8770$ g mol^{-1}, as shown in Figure 1). Some results regarding the structure and properties of the functionalized MWNTs (MWNT−LMCS) are also presented.

* Author to whom correspondence should be addressed. Phone: +86-27-8754-3261. Fax: +86-27-8754-3632. E-mail: hust_wcguan@yahoo.com.cn.

[†] Huazhong University of Science and Technology.

[‡] Guangzhou Institute of Chemistry.

[§] Wuhan University.

[||] Wuhan Institute of Physics and Mathematics.

10.1021/bm0604146 CCC: $37.00
Published on Web 01/04/2007

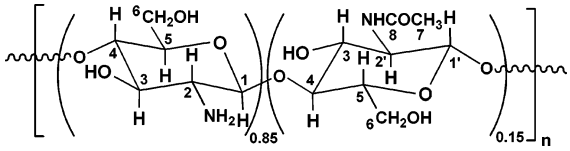

Figure 1. Chemical structure of the LMCS.

Experimental Section

Materials. MWNTs manufactured by CVD were purchased from Shenzhen Nanotech Port Co. (China). Prepared LMCS was obtained from Jinan Haidebei Marine Bioengineering Co. (China). The degree of deacetylation for the LMCS sample was determined to be 84.7%. Its $\bar{M}_w$ was determined to be 8770 g mol^{-1} by gel permeation chromatography (GPC). Hydrofluoric acid (40 wt %), LiCl (anhydrous, 95%), tetrahydrofuran (THF, 99%), dimethylformamide (DMF, 99%), $SOCl_2$ (99%), and pyridine (99%) were purchased from Shanghai Reagents Co. (China). Deuterated water, acetic acid, and dimethylsulfoxide (DMSO) for ^{1}H NMR measurements were obtained from Aldrich.

Preparation for Shortened MWNTs. MWNTs (4 g) were shortened using a planetary ball milling apparatus. The average length of the short nanotubes was measured by a LB-550 laser particle size analyzer to be 141 nm (Figure S1, Supporting Information).

Purification of the MWNTs. The shortened nanotubes were first sonicated and steeped in 24 wt % HF aqueous solution to eliminate SiO_2 and further purified by using HNO_3 and a surfactant OP-10.

Oxidation of the MWNTs. The purified MWNTs (3.420 g) were refluxed in a mixture of concentrated sulfuric acid (100 mL), nitric acid (40 mL), and distilled water (300 mL) for 24 h (final weight of MWNT−COOH, 2.516 g).

Preparation for MWNT−COCl. The oxidized MWNTs (2.516 g) in $SOCl_2$ (280 mL) together with DMF (3 mL) were refluxed for 52 h to convert the nanotube-bound carboxylic acids into acyl chlorides (final weight of MWNT−COCl, 2.761 g).[15]

Functionalization of the MWNTs with LMCS. In a typical experiment, carefully dried LMCS (3.587 g) and LiCl (2.457 g) were dispersed in DMF (260 mL), heated to 150 °C, and stirred under dried nitrogen for 2 h. After being cooled, MWNT−COCl (0.302 g) was added followed by 20 mL of pyridine. The mixture was sonicated for 1 h, then stirred, and refluxed under nitrogen for 48 h. Upon being cooled, the resultant mixture was filtered through a 0.22 μm pore size nylon membrane. A puce-colored filtrate was collected and taken to dryness on a rotary evaporator. Followed by a complete removal of solvent, the resulting black solid was stirred in distilled water (500 mL) for 6 h; by filtration again, a black residue was collected on the 0.22 μm pore size nylon filter, accompanied with a red-brown aqueous solution. The residue was sonicated in water (500 mL) for 1 h, filtered, washed with another 2500 mL of water, and then repeatedly extracted with water in a Soxhlet apparatus for 72 h. The final product was dried at 80 °C under vacuum for 24 h (weight of the MWNT−LMCS, 0.296 g).

Measurements. Fourier transform infrared (FTIR) spectra were recorded on a Bruker VERTEX 70 spectrometer from KBr pellets. ^{1}H NMR experiments were carried out on a Bruker DRX-400 spectrometer with resonance frequencies of 400 MHz. Solid-state ^{13}C cross-polarization magic-angle-spinning NMR experiments were performed at 9.4 T on a Varian Infinity Plus 400 spectrometer operating at a ^{13}C Larmor frequency of 100.4 MHz. ^{13}C chemical shifts were referenced to hexamethyl benzene. X-ray photoelectron spectroscopy (XPS) was conducted on a Kratos XSAM 800 spectrometer with a magnesium anode at 400 W, 15 kV, and 27 mA (Mg Kα 1253.6 eV, type 10-360 spherical capacitor analyzer). Transmission electron microscopy (TEM) images were obtained from a JEOL JEM-2010 operating at 200 kV. Thermogravimetric analysis (TGA) experiments were carried out on a Perkin-Elmer Pyris I TGA system with a typical heating rate of 10 °C min^{-1} in a N_2 atmosphere. Powder X-ray diffraction (XRD) patterns were recorded over a 2θ range of 5−90° by a PANalytical B. V. χ'Pert Pro using Cu Kα as an X-ray source and operating at 40 kV and 40 mA.

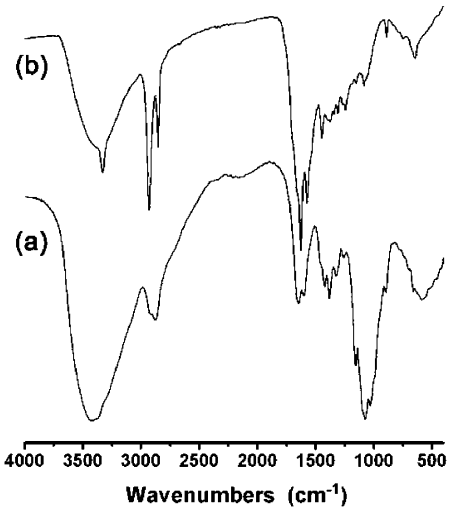

Figure 2. FTIR spectra of (a) the LMCS and (b) the MWNT−LMCS.

Results and Discussion

It should be noted that pristine MWNTs were first modified with the LMCS in our study to test the reaction between the MWNT−COCl and the chitosan. Although the reaction conditions were the same as that of the shortened MWNTs modified with the LMCS later, it was difficult to obtain enough products with improved solubility for further studies (less than 10 mg in each reaction). The cause may originate in the poor reactivity and dispersibility of the MWNTs. Pristine MWNTs are ranging from micrometers to millimeters, highly tangled, and insoluble any solvent; the tips of the nanotubes are usually closed. But the most reactive sites of the nanotubes are their open tips, defects, and curves.[16] By the cutting approach, the long and highly tangled nanotubes may be converted into short lengths of open tubes, fullerene pipes, so that they can be suspended, sorted, and manipulated as individual macromolecules.[16a] For example, shortened MWNTs can be dispersed in polar solvents more easily than crude MWNTs.[17a] So cutting may facilitate chemical reactions of the nanotubes. More importantly, shortened MWNTs are better candidates for adsorbent or graphite-like catalyst support than pristine MWNTs.[17b] Thus, the MWNTs were cut by ball milling and then functionalized with the LMCS.

After the reaction of the shortened MWNTs with the LMCS and separations, a black residue that was soluble in DMF but water insoluble and a red-brown aqueous solution were collected. By TEM imaging, both contained MWNTs. Although different dialysis membranes and ultrafiltering tubes were employed, it was very difficult to obtain the target product with perfect purity from the brown solution due to the physically adsorbed LMCS. Contrarily, the residue was conveniently separated from the LMCS by sonication and repeated extraction with water. Consequently, the purified single resultant, which was considered as the LMCS-functionalized MWNTs via the nucleophilic substitution reaction, was worthy of detailed investigation. However, confirmation of the covalent bonding between the attached LMCS and the MWNTs was complicated by (i) approximately 15% of the glucopyranose rings originally bearing amide groups, (ii) the presence of both primary and secondary hydroxyl groups, and (iii) the difficulty of satisfying structure interpretation of functionalized CNTs.[18] Thus, a comprehensive characterization was necessary.

In the FTIR spectrum of the MWNT−LMCS (Figure 2), two characteristic bands of the glucopyranose rings appear at approximately 893 and 1150 cm^{-1}, respectively, implying the

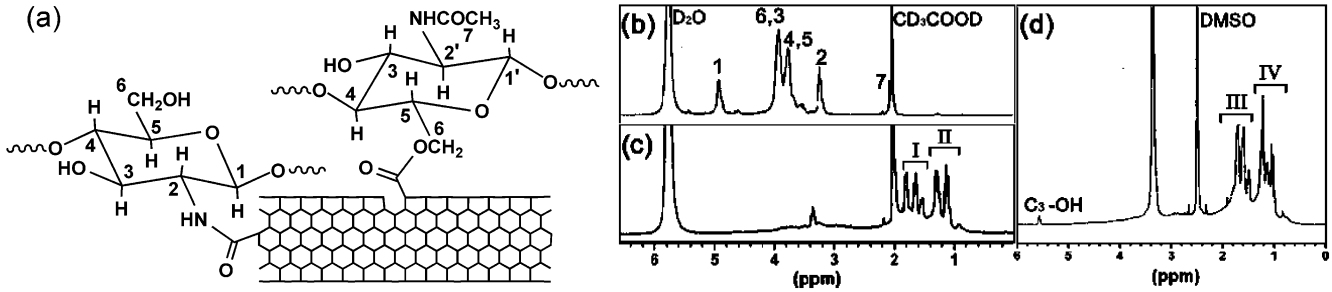

Figure 3. (a) Schematic representation for the glucopyranose rings attaching to the backbone of the MWNTs and ^{1}H NMR spectra of (b) the LMCS (CD_3COOD/D_2O, 1:1 (v/v)), (c) the MWNT−LMCS (CD_3COOD/D_2O, 1:1 (v/v)), and (d) the MWNT−LMCS (DMSO-d_6).

attachment of the LMCS.[19a,b] Moreover, a much stronger band occurs at 1628 cm^{-1} (amide I), and the 1602 cm^{-1} band, which was assigned to N−H bending in the amino and amide groups of the LMCS, was replaced by a new band at 1575 cm^{-1} (amide II), suggesting that some amino groups were converted into amide groups.[11,19b] In addition, the new bands at 1247 and 1190 cm^{-1} (C−O) as well as the very weak band at 1032 cm^{-1} suggest that the primary hydroxyl groups participated partly in the reaction.[19c,d] Furthermore, the broad O−H and N−H absorption band of the LMCS at approximately 3414 cm^{-1} shifted to 3328 cm^{-1} and became sharp, not only supporting the discussions above but also implying that hydrogen bonds have formed on the functionalized surface of the MWNTs.[19c,d]

To verify the findings from the FTIR spectra, XPS analysis was employed. For the MWNT−LMCS, the XPS survey spectrum presents all expected elements with the contents of 81.6 at. % (carbon), 11.0 at. % (oxygen), and 7.4 at. % (nitrogen). In comparison with MWNT−COCl, the increase of oxygen content arose from the attached LMCS.

In the C 1s spectrum of the MWNT−COCl, the higher binding energy of 291.2 eV can be assigned to acyl chloride groups.[20a] After functionalization, two signals with binding energies higher than 288.0 eV are present in the C 1s spectrum. The broad signal at 289.2 eV can be attributed to the ester carbon,[20b] indicating the formation of ester bonds. Although the C 1s peak at 288.5 eV is due to emission from the amide carbon,[20b] it is not sufficient for proving the formation of new amide bonds just by the C 1s XPS and FTIR spectra. This is further illuminated in the N 1s spectra. For the LMCS, two main N 1s peaks at 399.3 and 401.6 eV represent the $-NH_2$[11] and $-NH_3^+$ contributions,[20b] respectively. However, the N 1s spectrum of the MWNT−LMCS shows one predominant peak at 399.9 eV with a full width at half-maximum of 2.9 eV. N 1s binding energies for amides and amines are expected between 399.5 and 400.5 eV,[20c] and Liao et al. assigned the peak at 399.8 eV to the amide nitrogen.[20b] Thus, both the energy and the comparatively broad line width support the conversion of a part of amino into an amide.

NMR has been a useful tool to provide valuable information on the covalently functionalized CNTs.[18,21] And there are many precedents for complicated shifting of resonance signals in solid-state ^{13}C NMR and especially in solution-state ^{1}H NMR spectra of functionalized nanotubes.[18,21] The shifting of the resonances is consistent with experimental and theoretical works indicating a large diamagnetic susceptibility resulting from delocalized electrons (a π-electron ring current) in nanotubes.[21c]

As compared with the LMCS, the ^{13}C NMR spectrum of the MWNT−LMCS shows a characteristic ^{13}C nanotube resonance at 128 ppm[21c] and a new signal at 157 ppm, which further confirms the formation of ester bonds.[19c,d] Other identified resonances arising from the LMCS can be also observed,[22a] whereas the signals of C(1−6) are shifted upfield, especially for C(2) and C(6).

The chemical reactivity for the functional groups in chitosan generally follows the order: amino at C(2) > primary hydroxyl at C(6) > secondary hydroxyl at C(3).[22b] As for chloroacetylation of chitosan, both C(3) and C(6) are possible sites for esterification, whereas it was concluded that C(6) was the major substitution site.[22a] The fact that the signals shift further upfield indicates that C(2) and C(6) are even closer to the tubes and thus exposed to a stronger shielding caused by the surrounding π-system.[21c] All of these results suggest that the reaction mainly led to a covalent linkage between the LMCS and the MWNTs through amide and ester bonds, as depicted in Figure 3a.

More information on the structure of the MWNT−LMCS is illustrated in the ^{1}H NMR spectra (Figures 3b−d). In comparison with the proton signals of the LMCS (Figure 3b),[22a] the corresponding resonances of the MWNT−LMCS are shifted upfield considerably (Figure 3c), and the signals next to the solvent peak of CD_3COOD are divided into two groups (I and II). Taking into account that a portion of the glucopyranose rings are attaching directly to the backbone of the MWNTs and consequently the neighboring rings are "dragged" to the surface of the nanotubes, protons of these rings are even shielded. Therefore, signal group II that might be assigned to H(2−6) appears even upfield (1.01−1.31 ppm). On the contrary, group I consists of three broad signals ranging from 1.52 to 1.82 ppm, presumably corresponding to the H(6,3), H(4,5), and H(2) of the glucopyranose rings, respectively, which are relatively far from the nanotubes. Similarly, resonances of the MWNT−LMCS in DMSO-d_6 (Figure 3d) also comprise two signal groups (III and IV). The integrated area of group III is approximately equal to that of group IV, and the same is true of groups I and II, implying that approximately one-half of the total glucopyranose rings are very close to the nanotubes. Additionally, disappearance of the double peaks at 5.56 and 5.74 ppm in Figure 3d with the addition of D_2O is attributed to the secondary hydroxyl groups in the MWNT−LMCS.[19d]

The LMCS-functionalized MWNTs are also verified by TEM imaging. It depicts representative features showing the shortened MWNTs coated with an amorphous polymeric material, as marked by the arrows (Figure 4c). As the MWNT−LMCS was extracted with water for 72 h, any physically absorbed substance like LMCS should be removed previously, and the material surrounding the nanotubes is deduced to be the attached LMCS moieties.

By TGA analysis, the LMCS content in the MWNT−LMCS is approximately 58 wt %. Furthermore, the XPS data yield a nitrogen-to-carbon ratio of 0.091, which enables us to give an estimate of the average degree of functionalization in the MWNT−LMCS sample. On the basis of the chemical formula and $\bar{M}_w$ of the LMCS, it is calculated that approximately four

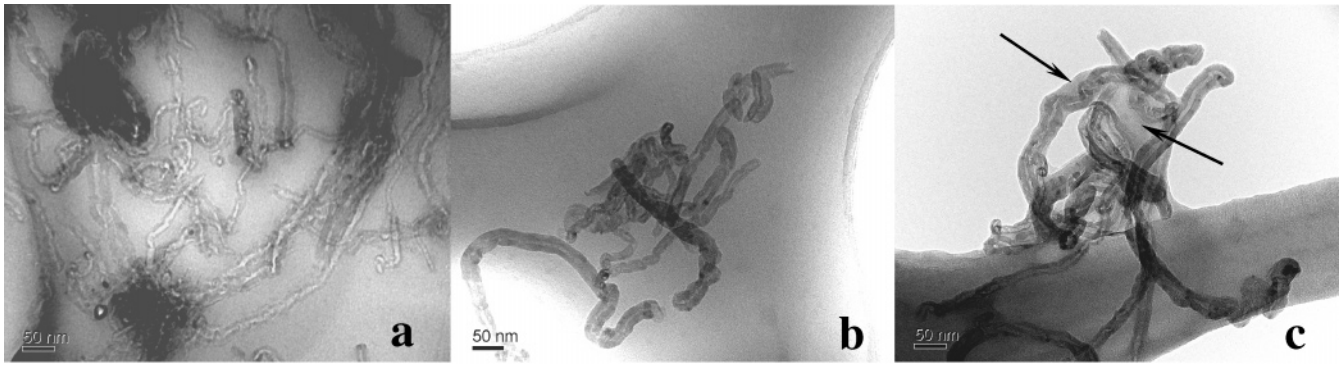

Figure 4. TEM images of (a) raw MWNTs, (b) cut and purified MWNTs, and (c) the MWNT−LMCS. Arrows indicate the typical features of the attached LMCS.

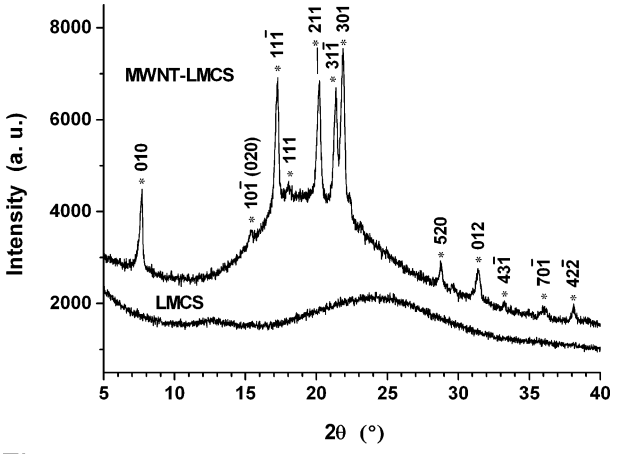

Figure 5. XRD plots for the LMCS and MWNT−LMCS.

molecular chains of the LMCS are attached to 1000 carbon atoms of the nanotube sidewalls.

Powder XRD spectra of the LMCS and the MWNT−LMCS are shown in Figure 5. The LMCS exhibits only one broad and weak peak around 24°. Most interestingly, 12 crystalline reflections can be observed in the 2θ range of 5−40° for the functionalized MWNTs. As it is known, CNTs exhibit only one characteristic peak around 26° between 5° and 40°.[23] And studies have shown that, as for nanotubes modified with polymers and nanotubes in composites, the peak around 26° decreased in intensity or even disappeared, whereas the precise reasons remain unknown.[23] Although the MWNT−LMCS does not show a distinct peak around 26°, it ensures that the new diffraction spots cannot be attributed to the MWNTs. Alternately, comparisons of the XRD data of the MWNT−LMCS with that of chitosan indicate that the new reflections are relevant to chitosan.[24a,25a] That is, the amorphous packing structure of the LMCS changed dramatically when it attached to the MWNTs.

It should be mentioned that the crystallinity and polymorphism of chitosan are affected by chitosan origin, molecular weight, water molecules, inorganic or organic acids, and annealing, etc.[24] The lower crystallinity of the LMCS could be ascribed to its low molecular weight. In addition, chemical modification can also affect the crystallinity of chitosan. A case in point is the increased crystallinity of *N*-phthaloyl-chitosan.[25b] Then, what caused the crystallinity of the attached LMCS, which possesses approximately 58 wt % of the MWNT−LMCS? Additional experiments showed that the crystallinity of the LMCS was little affected by recrystallization, and the crystallinity of the MWNT−LMCS was irrelevant to the water of hydration (Supporting Information).

Table 1. Solubility of the LMCS and MWNT−LMCS in a Variety of Solvents[a]

solvents	LMCS	MWNT−LMCS
distilled water	+	−
hydrochloric acid [b]	+	−
acetic acid [c]	+	+
dimethylsulfoxide	−	+
N,*N*′-dimethylformamide	−	+
N,*N*′-dimethyl acetamide	−	+

[a] Solubility: +, soluble; −, not soluble. [b] Hydrochloric acid: 1−35 wt % aqueous solution. [c] Acetic acid: 10−95 wt % aqueous solution.

As the most reactive sites of the nanotubes are their open tips, defects, and curves, the MWNTs were cut and highly oxidized before functionalization, which have been proved by the TEM imaging and oxygen content of the MWNT−COCl (6.2 at. %), respectively. With the increase of the reaction sites, it is possible that some reactive regions might form in the nanotube sidewalls. Consequently, molecular chains of the LMCS may tend to attach to these reactive regions, which might be conducive to the formation of intramolecular hydrogen bonds. Furthermore, as Wang et al. demonstrated, chitosan possesses a large number of amino and hydroxyl groups, and the oxidized MWNTs contain carboxylic groups; thus strong hydrogen bonding may be formed between the glucopyranose rings and the functional nanotubes.[25c] This might contribute to a relatively ordered arrangement of the attached molecular chains along the rigid tube sidewalls.

Since 2002, studies on polymer crystallization induced by CNTs have been reported, including polypropylene,[26a] poly(vinyl alcohol),[26b] R-BAPB-type thermoplastic polyimide,[26c] and poly(ethylene 2,6-naphthalate),[26d] etc. Most recently, Haggenmueller et al. demonstrated that SWNT bundles templated polyethylene (PE) crystallization with the PE chains parallel to the single-walled carbon nanotube axis.[27] On the basis of the discussions above, it is possible that covalent and noncovalent interactions caused the crystallization of attached LMCS chains on the rigid template offered by MWNTs. With respect to the amorphous LMCS, in other words, the MWNTs might induce the crystalline character of the attached LMCS.

Unlike the LMCS, the MWNT−LMCS is insoluble in pure water due to the increase in crystallinity, whereas it is easily soluble in DMSO, DMF, and dimethyl acetamide (DMAc) (Table 1). Also, it is soluble in acetic acid aqueous solution, which makes it possible to mix the MWNT−LMCS together with different chitosan matrixes in homogeneous systems in the next application step.

Conclusion

In summary, an efficient covalent functionalization of the MWNTs with the LMCS, an attractive green and natural polymer, via a nucleophilic substitution reaction, has been demonstrated. Amino and primary hydroxyl groups of the LMCS contributed mainly to the formation of MWNT−LMCS conjugates. The LMCS content in the MWNT−LMCS is approximately 58 wt %, and approximately four molecular chains of the LMCS are attached to 1000 carbon atoms of the nanotube sidewalls. Furthermore, the MWNTs might induce the crystalline character of the attached LMCS. As a novel derivative of MWNTs, the MWNT−LMCS is soluble in DMSO, DMF, DMAc, and acetic acid aqueous solution. The confirmation of the chitosan-based covalent functionalization route might lead to further studies aiming for potential applications in catalysis and environmental protection.

Acknowledgment. This work is supported by the National Natural Science Foundation of China (Grant No. 50374039).

Supporting Information Available. Experimental details, FTIR spectra, ^{13}C NMR spectra, ^{1}H NMR spectra, XPS spectra, TGA data, XRD data, and a method for calculating average number of the attached molecular chains. This material is available free of charge via the Internet at http://pubs.acs.org.

References and Notes

(1) (a) He, P.; Urban, M. W. *Biomacromolecules* **2005**, *6*, 2455. (b) Yoon, S. H.; Jin, H.-J.; Kook, M. C.; Pyun, Y. R. *Biomacromolecules* **2006**, *7*, 1280.
(2) Hill, D. E.; Lin, Y.; Rao, A. M.; Allard, L. F.; Sun, Y. P. *Macromolecules* **2002**, *35*, 9466.
(3) Qin, S. H.; Qin, D. Q.; Ford, W. T.; Resasco, D. E.; Herrera, J. E. *J. Am. Chem. Soc.* **2004**, *126*, 170.
(4) Xu, Y. Y.; Gao, C.; Kong, H.; Yan, D. Y.; Jin, Y. Z.; Watts, P. C. P. *Macromolecules* **2004**, *37*, 8846.
(5) Li, H. M.; Cheng, F. Y.; Duft, A. M.; Adronov, A. *J. Am. Chem. Soc.* **2005**, *127*, 14518.
(6) Feng, W.; Bai, X. D.; Lian, Y. Q.; Liang, J.; Wang, X. G.; Yoshino, K. *Carbon* **2003**, *41*, 1551.
(7) Jenkins, D. W.; Hudson, S. M. *Chem. Rev.* **2001**, *101*, 3249.
(8) Kumar, M. N. V. R.; Muzzarelli, R. A. A.; Muzzarelli, C.; Sashiwa, H.; Domb, A. J. *Chem. Rev.* **2004**, *104*, 6018.
(9) Varma, A. J.; Deshpande, S. V.; Kennedy, J. F. *Carbohydr. Polym.* **2004**, *55*, 77.
(10) Welsh, E. R.; Schauer, C. L.; Qadri, S. B.; Price, R. R. *Biomacromolecules* **2002**, *3*, 1370.
(11) Jin, L.; Bai, R. B. *Langmuir* **2002**, *18*, 9765.
(12) Esumi, K.; Takei, N.; Yoshimura, T. *Colloids Surf., B* **2003**, *32*, 117.
(13) (a) Li, Y. H.; Wang, S. G.; Luan, Z. K.; Ding, J.; Xu, C. L.; Wu, D. H. *Carbon* **2003**, *41*, 1057. (b) Li, Y. H.; Wang, S. G.; Wei, J. Q.; Zhang, X. F.; Xu, C. L.; Luan, Z. K.; Wu, D. H.; Wei, B. Q. *Chem. Phys. Lett.* **2002**, *357*, 263.
(14) (a) Philippe, S.; Massimiliano, C.; Philippe, K. *Appl. Catal., A* **2003**, *253*, 337. (b) He, Z. B.; Chen, J. H.; Liu, D. Y.; Tang, H.; Deng, W.; Kuang, Y. F. *Mater. Chem. Phys.* **2004**, *85*, 396.
(15) Chen, J.; Hamon, M. A.; Hu, H.; Chen, Y.; Rao, A. M.; Eklund, P. C.; Haddon, R. C. *Science* **1998**, *282*, 95.
(16) (a) Liu, J.; Rinzler, A. G.; Dai, H.; Hafner, J. H.; Bradley, R. K.; Boul, P. J.; Lu, A.; Iverson, T.; Shelimov, K.; Huffman, C. B.; Rodriguez-Macias, F.; Shon, Y.-S.; Lee, T. R.; Colbert, D. T.; Smalley, R. E. *Science* **1998**, *280*, 1253−1255. (b) Chen, J.; Dyer, M. J.; Yu, M. F. *J. Am. Chem. Soc.* **2001**, *123*, 6201.
(17) (a) Saito, T.; Matsushige, K.; Tanaka, K. *Physica B* **2002**, *323*, 280. (b) Niesz, K.; Siska, A.; Vesselényi, I.; Hernadi, K.; Méhn, D.; Galbács, G.; Kónya, Z.; Kiricsi, I. *Catal. Today* **2002**, *76*, 3.
(18) Holzinger, M.; Abraham, J.; Whelan, P.; Graupner, R.; Ley, L.; Hennrich, F.; Kappes, M.; Hirsch, A. *J. Am. Chem. Soc.* **2003**, *125*, 8574.
(19) (a) Pearson, F. G.; Marchessault, R. H.; Liang, C. Y. *J. Polym. Sci.* **1960**, *43*, 101. (b) Mi, F. L. *Biomacromolecules* **2005**, *6*, 980. (c) Pretsch, E.; Bühlmann, P.; Affolter, C. *Structure Determination of Organic Compounds: Tables of Special Data*, 3rd ed.; Springer-Verlag: Berlin, 2000. (d) Ning, Y. C. *Structural Identification of Organic Compounds and Organic Spectroscopy*, 2nd ed.; Science Press: Beijing, 2000.
(20) (a) Wagner, C. D.; Naumkin, A. V.; Kraut-Vass, A.; Allison, J. W.; Powell, C. J.; Rumble, J. R. J. *National Institute of Standards and Technology X-ray Photoelectron Spectroscopy Database*, version 3.4; National Institute of Standards and Technology: Gaithersburg, MD, 2003. (b) Liao, J. D.; Lin, S. P.; Wu, Y. T. *Biomacromolecules* **2005**, *6*, 395. (c) Ramanathan, T.; Fisher, F. T.; Ruoff, R. S.; Brinson, L. C. *Chem. Mater.* **2005**, *17*, 1294.
(21) (a) Tang, X. P.; Kleinhammes, A.; Shimoda, H.; Fleming, L.; Bennoune, K. Y.; Sinha, S.; Bower, C.; Zhou, O.; Wu, Y. *Science* **2000**, *288*, 492. (b) Cahill, L. S.; Yao, Z.; Adronov, A.; Penner, J.; Moonoosawmy, K. R.; Kruse, P.; Goward, G. R. *J. Phys. Chem. B* **2004**, *108*, 11415. (c) Peng, H. Q.; Alemany, L. B.; Margrave, J. L.; Khabashesku, V. N. *J. Am. Chem. Soc.* **2003**, *125*, 15180.
(22) (a) Sashiwa, H.; Kawasaki, N.; Nakayama, A.; Muraki, E.; Yamamoto, N.; Zhu, H.; Nagano, H.; Omura, Y.; Saimoto, H.; Shigemasa, Y.; Aiba, S. *Biomacromolecules* **2002**, *3*, 1121. (b) Yoksan, R.; Akashi, M.; Biramontri, S.; Chirachanchai, S. *Biomacromolecules* **2001**, *2*, 1038.
(23) (a) Guo, H.; Sreekumar, T. V.; Liu, T.; Minus, M.; Kumar, S. *Polymer* **2005**, *46*, 3001. (b) Feng, W.; Bai, X. D.; Lian, Y. Q.; Liang, J.; Wang, X. G.; Yoshino, K. *Carbon* **2003**, *41*, 1551. (c) McNally, T.; Pötschke, P.; Halley, P.; Murphy, M.; Martin, D.; Bell, S. E. J.; Brennan, G. P.; Bein, D.; Lemoine, P.; Quinn, J. P. *Polymer* **2005**, *46*, 8222. (d) Wang, F. X.; Gao, X. P.; Lu, Z. W.; Ye, S. H.; Qu, J. Q.; Wu, F.; Yuan, H. T.; Song, D. Y. *J. Alloys Compd.* **2004**, *370*, 326. (e) Shan, Y.; Gao, L. *Nanotechnology* **2005**, *16*, 625.
(24) (a) Ogawa, K.; Hirano, S.; Miyanishi, T.; Yui, T.; Watanabe, T. *Macromolecules* **1984**, *17*, 973. (b) Saitô, H.; Ryoko, T.; Ogawa, K. *Macromolecules* **1987**, *20*, 2425.
(25) (a) Ye, X.; Kennedy, J. F.; Li, B.; Xie, B. J. *Carbohydr. Polym.* **2006**, *64*, 532. (b) Kurita, K.; Ikeda, H.; Yoshida, Y.; Shimojoh, M.; Harata, M. *Biomacromolecules* **2002**, *3*, 1. (c) Wang, S. F.; Shen, L.; Zhang, W. D.; Tong, Y. J. *Biomacromolecules* **2005**, *6*, 3067.
(26) (a) Grady, B. P.; Pompeo, F.; Shambaugh, R. L.; Resasco, D. E. *J. Phys. Chem. B* **2002**, *106*, 5852. (b) Probst, O.; Moore, E. M.; Resasco, D. E.; Grady, B. P. *Polymer* **2004**, *45*, 4437. (c) Vladimir, E. Y.; Valentine, M. S.; Alexander, N. S.; Dmitriy, G. L.; Alexander, Y. F.; Gad, M. *Macromol. Rapid Commun.* **2005**, *26*, 885. (d) Kim, J. Y.; Park, H. S.; Kim, S. H. *Polymer* **2006**, *47*, 1379.
(27) Haggenmueller, R.; Fischer, J. E.; Winey, K. I. *Macromolecules* **2006**, *39*, 2964.

BM0604146